Supplemental Information

This file includes:
Materials and Methods
Figs. S1 to S3
Tables S1 and S2
References

Materials and Methods

Additional methods for cropland mapping

Figure S1 summarizes our workflow and validation methods for developing the cropland dataset used in this study. To generate this dataset, we integrated five different data products using a synthesis approach to generate our cropland extent estimate. We included the hybrid land cover product produced by the IIASA/IFPRI Geo-Wiki project, though it is a temporal outlier (nominal year 2005), in the generation of our cropland dataset because of its unique utilization of crowd-sourced data for training and validation. Though this data also utilizes the MODIS land cover data as part of the hybridized product, the data are temporally distinct (2005 vs 2010-2015) and are modified by the classification approach used in the generation of the dataset. Because the MODIS LC product is produced annually we include multiple time steps to minimize inter-annual variation in cropland estimates.

We validated our cropland dataset using two different methods. First, we compared our estimates of country cropland area to FAO mean country cropland area for 2010-2016 (1). We evaluated accuracy using the GAUL country dataset to better harmonize with FAO country definitions (r^2=.98) (Fig. S1B), though accuracy was also high (r^2=.95) using the GADM country boundaries used in the rest of the study. We also evaluated spatial accuracy using cropland validation data collected through the second campaign of the Geo-Wiki project (2), these data are independent of data used for training and validation in the IIASA/IFPRI hybrid land cover used to create our cropland dataset. To avoid issues of quality control, we used a subset of 1,853 validation points collected by students trained in satellite image interpretation and experts. Using these data, we plotted an ROC and calculate the AUC using a trapezoidal approximation, giving a value of 0.87 (Fig. S1C). This suggests good threshold invariant accuracy for our data. Because our data are continuous, depicting subpixel proportions of cropland, evaluating these data using a single binary threshold is not appropriate, hence our reporting of the AUC and presentation of the ROC curve for interpretation.

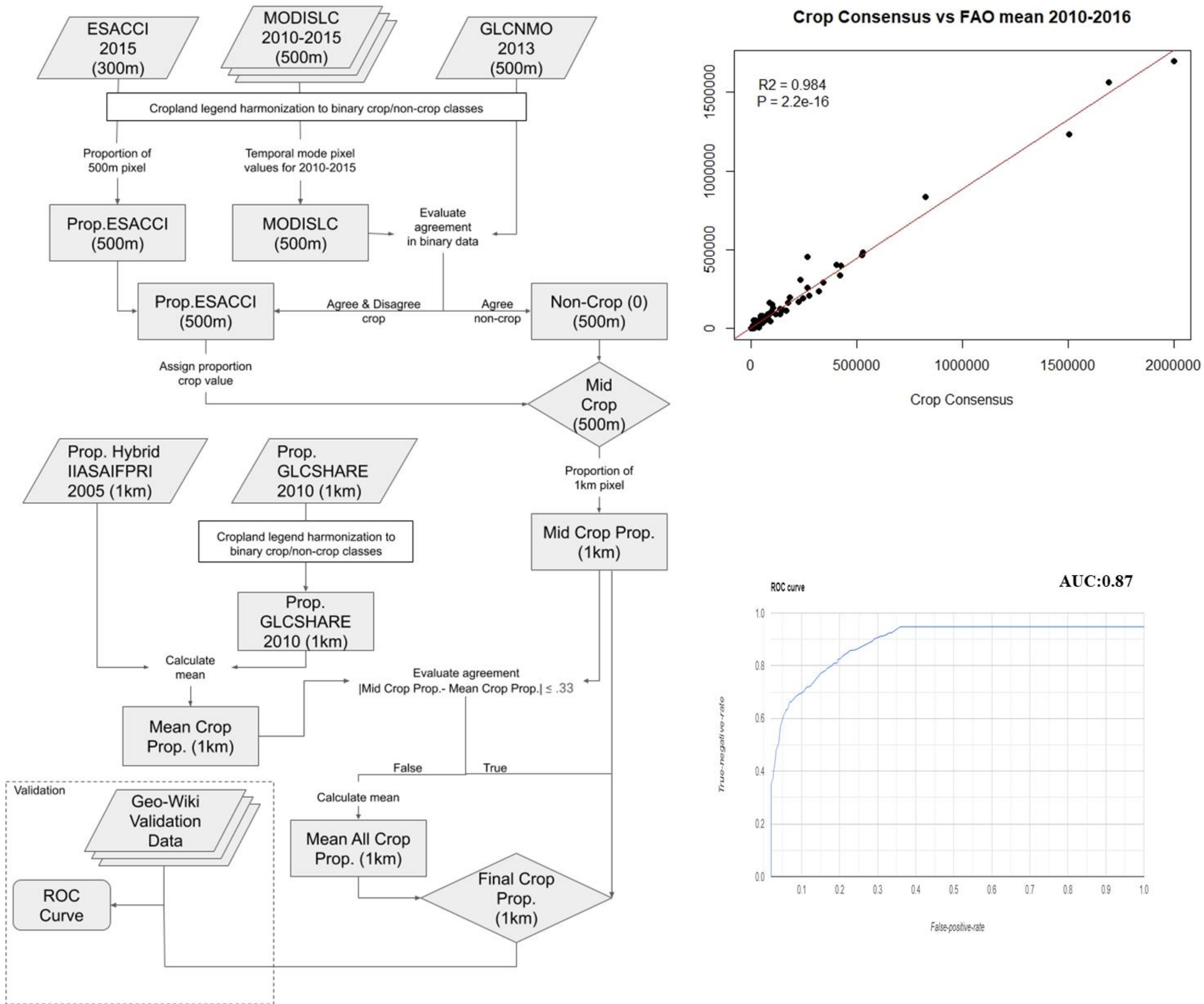

Fig. S1. (*A*) Data processing workflow (*B*) Crop area by country (this study) vs FAO crop area by country (*C*) ROC curve depicting accuracy of crop data (this study) based on GeoWiki validation data. Validation analysis was carried out in Google Earth Engine.

Predictor Variables	Source (Citation)	Hypothesis
Country Area	GADM, Database of Global Administrative Areas (3)	Geometric constraint included in base model
Total Protected Area	World Database on Protected Areas (4)	geometric constraint included in base model
Total Cropland Area	Consensus Cropland (this study)	geometric constraint included in base model
Gini Index	World Bank (5), CIA (6), World Income Inequality Database (7)	higher income inequality increases pressure for cropland production in protected area
Human Pop. Density	Gridded Population of the World (8)	higher human population density increases pressure for cropland production in protected area
Proportion of GDP in Agriculture	World Bank (5), CIA (6)	greater economic reliance on agriculture increases pressure for cropland production in protected area
Agricultural Suitability in Protected Area	Zabel et al. (9)	higher agricultural suitability in protected area increases likelihood of cropland production in protected area
Self-Sufficiency Ratio	FAO Food Balance Sheets (1)	higher reliance on domestic food production increases pressure for cropland production in protected area
Mean Year of Protection	World Database on Protected Areas (4)	newer protected areas tend to have less cropland and are more likely to be sited in intact areas

Table S1. Model predictors of cropland inside protected area and relevant hypotheses.

Additional methods for country level predictors

GINI index is calculated using the most recent estimate of GINI index as provided by World Income Inequality Database. Where no estimate was available we use the mean of the most recent estimates by the World Bank and CIA. Proportion of GDP in Agriculture is calculated as the mean of World Bank estimates from 2000 to 2017. Where World Bank estimates were not available we used the most recent estimates by the CIA. Self Sufficiency Ratio is calculated from FAO Food Balance Sheets by (SSR) = production x 100/ (production + imports - exports).

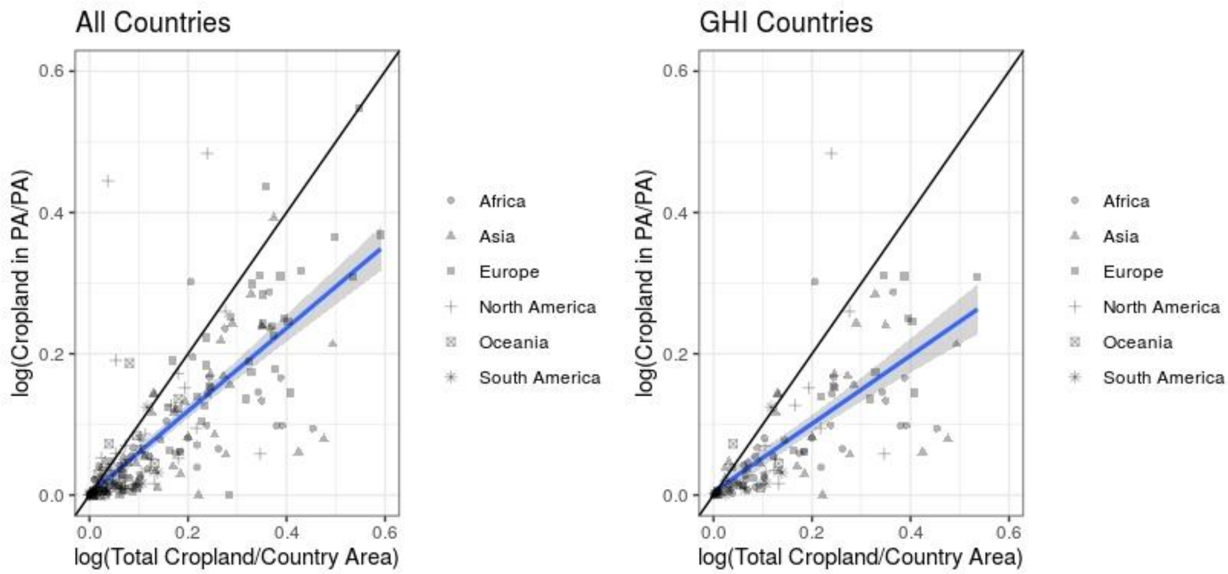

Fig. S2. Null models for all countries and GHI subsample evaluating random distribution of cropland in PA, total PA, total cropland area, and country area.

Null Model results

The 1:1 line shown in black represents the null expectation of random distribution of cropland in protected area relative to the proportion of cropland in the country. A linear model fit to these data (shown in blue with 95% CI in gray) shows that both in the global dataset and in GHI countries, cropland in protected areas occurs less than would be expected, particularly in countries with a greater fraction of total cropland. For this reason, we used a more flexible model specification (Eqns. 2 and 3 in main text) when seeking to test our hypotheses about the role of covariates (Table S1).

Predictor	**Global Model Estimate (Adj. SE)**	**Global Model SW**	**Hunger Model Estimate (Adj. SE)**	**Hunger Model SW**
Country Area	-0.58 (0.11)	1.00	-0.60 (0.13)	1.00
Total Protected Area	0.86 (0.07)	1.00	0.88 (0.08)	1.00
Total Cropland	0.70 (0.07)	1.00	0.66 (0.09)	1.00
Human Population Density	0.35 (0.14)	1.00	0.24 (0.18)	0.80
Agricultural Suitability in Protected Areas	0.27 (0.11)	1.00	0.09 (0.12)	0.47
GINI Index	-0.21(0.08)	1.00	-0.14 (0.12)	0.76

Table S2. Predictor estimates (not standardized for three base model estimates shown first), adjusted standard error (SE) and sum of Akaike weights (SW) for global and hunger subset model average.

Additional Regression Methods and Results

We constructed models for all possible combinations of these covariates while always controlling for the effects of country area, total protected area and total cropland area, retaining those having AIC values to within 2 units of the minimum AIC value that we observed. The Global ensemble model was constructed from an average of top four linear models meeting inclusion criteria of Δ AICc ≤ 2. For the subset monitored by the Global Hunger Index, the final ensemble model was constructed from an average of seven models meeting inclusion criteria of Δ AICc ≤ 2.

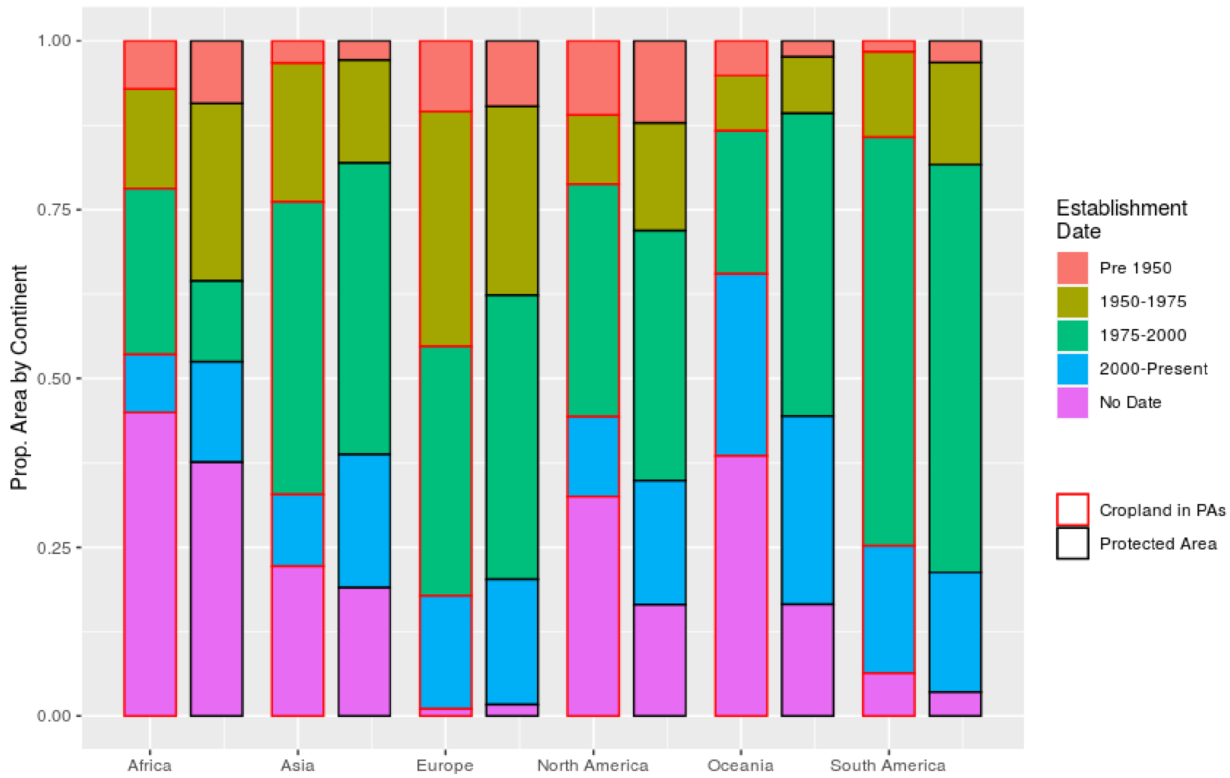

Fig. S3. Proportion of cropland and protected area in each age class by continent. Stacked bars outlined in red show proportions of cropland in protected area by age class and bars outline in black show proportions of protected area by age class.

In Europe, almost half (.45) of cropland in protected areas is found in areas established by 1975, occurring disproportionately with respect to patterns of protected area siting. In other continents, a smaller proportion is found in older protected areas, though establishment dates are not recorded for all areas. This can be observed in patterns of cropland occurrence in South America and in Africa (mean recorded establishment date = 1982) where more recent (post 1975) areas are more prone to cropland impacts. The distributions of cropland by protected area establishment date was significantly different between continents (chi-square, $\chi^2 = 366138$, df = 20, $p < .001$).

References

1. F. Faostat, Food and agriculture data., 2019 (2019).

2. J. C. Laso Bayas, *et al.*, A global reference database of crowdsourced cropland data collected using the Geo-Wiki platform. *Scientific Data* **4**, 170136 (2017).

3. G. A. Areas, GADM Database of Global Administrative Areas, version 2.8. 2015. *URL http://www. gadm. org* (2019).

4. I. UNEP-WCMC, Protected Planet: the World Database on Protected Areas (WDPA), the Global Database on Protected Areas Management Effectiveness (GD-PAME) (2019).

5. World Bank, World Development Indicators (2019).

6. Central Intelligence Agency, *The CIA world factbook* (2019).

7. F. Solt, Measuring income inequality across countries and over time: The standardized world income inequality database (2019).

8. (CIESIN) Center for International Earth Science Information Network-Columbia University, Gridded population of the World, version 4 (GPWv4) revision 11 (2018).

9. F. Zabel, B. Putzenlechner, W. Mauser, Global agricultural land resources–a high resolution suitability evaluation and its perspectives until 2100 under climate change conditions. *PloS one* **9** (2014).